

least one constituent of the product has a limited solubility in it. Under our reaction conditions, indium metal (m.p. 157°C) is indeed molten and dissolves less than 0.001 atomic % nitrogen.<sup>[13]</sup> The most obvious characteristics of the VLS<sup>[12]</sup> and SLS<sup>[5, 6]</sup> mechanisms—one-dimensional fiber or whisker growth morphologies and attached metal-catalyst particles—were clearly evident in the InN samples produced. Consequently, all the key indicators of the SLS growth mechanism were present.

The SLS growth process has been previously demonstrated for group III element phosphides and arsenides,<sup>[5, 6]</sup> which are thermally stable at conventional growth temperatures. However, indium nitride is not. The SLS mechanism operates at very low temperatures in comparison to conventional materials-synthesis methods, presumably because it is catalytic and lowers energy barriers for both precursor decomposition and the interfacial steps required for nonmolecular crystal growth (crystal lattice assembly). SLS synthesis of other thermally unstable compounds and crystal structures should be possible.

### Experimental Section

Compounds  $t\text{Bu}_3\text{In}^{[14]}$  and  $i\text{Pr}_3\text{In}^{[15]}$  were prepared according to the literature. The synthesis of  $t\text{Bu}_3\text{InN}_3$  (**1b**) is described here;  $i\text{Pr}_3\text{InN}_3$  (**1a**) was prepared similarly. MeOH (225  $\mu\text{L}$ , 0.178 g, 5.55 mmol) was added to a dry,  $\text{O}_2$ -free solution of  $t\text{Bu}_3\text{In}$  (1.61 g, 5.63 mmol) in hexane (20 mL) at 25°C. The mixture was stirred for 10 min and then  $\text{N}_3\text{SiMe}_3$  (0.800 mL, 0.660 g, 5.73 mmol) was added, instantly generating a fine white precipitate. The slurry was stirred for 2 h. Precursor **1b** was then collected by filtration and washed with  $2 \times 5$  mL of hexane (yield: 1.39 g, 5.12 mmol, 91 %). Analytical data for **1b**: m.p. 210°C (dec.); elemental analysis calcd for  $\text{C}_8\text{H}_{18}\text{InN}_3$ : C 35.45, H 6.69, N 15.50; found: C 35.74, H 6.46, N 15.44;  $^1\text{H}$  NMR ( $[\text{D}_6]\text{acetone}$ ):  $\delta = 1.29$  (s, 18H); IR (KBr):  $\tilde{\nu} = 2087\text{ cm}^{-1}$  (asym.  $\text{N}_3$ ). Analytical data for **1a**: m.p. 181°C;  $^1\text{H}$  NMR ( $[\text{D}_5]\text{pyridine}$ ):  $\delta = 1.34$  (d, 12H,  $J = 6.6\text{ Hz}$ ), 1.45 (m, 2H); IR (KBr):  $\tilde{\nu} = 2075\text{ cm}^{-1}$  (asym.  $\text{N}_3$ ). In a typical InN synthesis, **1a** or **1b** (1.5 mmol) and 1,1-dimethylhydrazine (3.0 mmol) were combined in dry,  $\text{O}_2$ -free 1,3-diisopropylbenzene (10 mL) at 25°C. The mixture was stirred for 2 h, then heated to reflux at 203°C (in a sand bath under an efficient condenser) for 20 h. The resulting, air-stable InN/In product was collected by filtration and washed with  $2 \times 10$  mL of pentane (yield: 90–95 %). Elemental analysis calcd for InN: C 0, H 0, N 10.88, In 89.13; found (from **1a**): C 1.87, H 0.12, N 7.31, In 84.1; found (from **1b**): C 2.05, H 0.19, N 8.39, In 81.6.

Received: April 18, 1999

Revised: January 17, 2000 [Z13328]

- [1] a) T. Matsuoka, *Adv. Mater.* **1996**, *8*, 469–479; b) F. A. Ponce, D. P. Bour, *Nature* **1997**, *386*, 351–359; c) S. Nakamura, *Science* **1998**, *281*, 956–961.
- [2] a) D. A. Neumayer, J. G. Ekerdt, *Chem. Mater.* **1996**, *8*, 9–25; b) A. C. Jones, C. R. Whitehouse, J. S. Roberts, *Chem. Vap. Deposition* **1995**, *1*, 65–74; c) I. Akasaki, H. Amano, *J. Crystal Growth* **1995**, *146*, 455–461.
- [3] I. Grzegory, J. Jun, M. Bockowski, St. Krukowski, M. Wróblewski, B. Lucznik, S. Porowski, *J. Phys. Chem. Solids* **1995**, *56*, 639–647.
- [4] R. A. Fischer, A. Miehr, T. Metzger, E. Born, O. Ambacher, H. Angerer, R. Dimitrov, *Chem. Mater.* **1996**, *8*, 1356–1359.
- [5] W. E. Buhro, K. H. Hickman, T. J. Trentler, *Adv. Mater.* **1996**, *8*, 685–688.
- [6] a) T. J. Trentler, K. M. Hickman, S. C. Goel, A. M. Viano, P. C. Gibbons, W. E. Buhro, *Science* **1995**, *270*, 1791–1794; b) T. J. Trentler, S. C. Goel, K. M. Hickman, A. M. Viano, M. Y. Chiang, A. M. Beatty, P. C. Gibbons, W. E. Buhro, *J. Am. Chem. Soc.* **1997**, *119*, 2172–2181.

- [7] a) J. Kouvetakis, D. B. Beach, *Chem. Mater.* **1989**, *1*, 476–478; b) K.-L. Ho, K. F. Jensen, J.-W. Hwang, W. L. Gladfelter, J. F. Evans, *J. Crystal Growth* **1991**, *107*, 376–380.
- [8] Crystallographic data for **1a**:  $\text{C}_{12}\text{H}_{28}\text{In}_2\text{N}_6$ , monoclinic, space group  $P2_1/c$ ,  $a = 8.1680(4)$ ,  $b = 17.6617(10)$ ,  $c = 6.8694(4)$  Å,  $\beta = 102.689(4)^\circ$ ,  $V = 966.78(9)$  Å<sup>3</sup>,  $Z = 2$ , 22 463 reflections collected, 2405 unique, final  $R_1(F) = 0.0184$ , final  $R_w(F^2) = 0.0446$  for 147 parameters, max./min. residual electron density =  $0.70/-0.81\text{ e Å}^{-3}$ . Crystallographic data for **1b**:  $\text{C}_8\text{H}_{18}\text{InN}_3$ , triclinic, space group  $P\bar{1}$ ,  $a = 6.8686(1)$ ,  $b = 9.5258(1)$ ,  $c = 9.9383(1)$  Å,  $\alpha = 79.536(1)$ ,  $\beta = 85.24$ ,  $\gamma = 70.428(1)^\circ$ ,  $V = 602.32(1)$  Å<sup>3</sup>,  $Z = 2$ , 13 486 reflections collected, 2885 unique, final  $R_1(F) = 0.0349$ , final  $R_w(F^2) = 0.0826$  for 109 parameters, max./min. residual electron density =  $1.40/-1.16\text{ e Å}^{-3}$ . Both data sets were collected using  $\text{MoK}\alpha$  radiation ( $\lambda = 0.71073$  Å) at 223(2) K with a Bruker SMART CCD Diffractometer. Full matrix refinement was conducted on  $F^2$  and H atoms were refined for **1a**. Details of the X-ray diffraction studies will be published elsewhere. Crystallographic data (excluding structure factors) for the structures reported in this paper have been deposited with the Cambridge Crystallographic Data Centre as supplementary publication no. CCDC-119361 (**1a**) and -119362 (**1b**). Copies of the data can be obtained free of charge on application to CCDC, 12 Union Road, Cambridge CB2 1EZ, UK (fax: (+44) 1223-336-033; e-mail: deposit@ccdc.cam.ac.uk).
- [9] P. A. S. Smith, *Derivatives of Hydrazine and Other Hydronitrogens Having N–N Bonds*, Benjamin/Cummings, Readings, **1983**, p. 20.
- [10] A. R. West, *Solid State Chemistry and its Applications*, Wiley, New York, **1984**, p. 174.
- [11] JCPDS card 02-1450 (indium nitride).
- [12] R. S. Wagner in *Whisker Technology* (Ed.: A. P. Levitt), Wiley, New York, **1970**, chap. 3.
- [13] S. Porowski, I. Grzegory, *EMIS Datarev. Ser.* **1994**, *11*, 82–85.
- [14] D. C. Bradley, D. M. Frigo, M. B. Hursthouse, B. Hussain, *Organometallics* **1988**, *7*, 1112–1115.
- [15] B. Neumueller, *Chem. Ber.* **1989**, *122*, 2283–2287.

## Oxidation–Reduction and Photochemical Reactions of Metalladecaborane Clusters: The Interconversion of *hypercloso*- $[(\eta^6\text{-C}_6\text{Me}_6)\text{RuB}_9\text{H}_9]$ and *closo*- $[(\eta^6\text{-C}_6\text{Me}_6)\text{RuB}_9\text{H}_9]^{2-}$

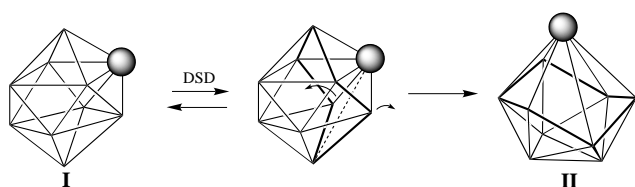
Ralf Littger, Ulrich Englisch, Karin Ruhlandt-Senge, and James T. Spencer\*

The most common structure for a 10-vertex polyhedral cluster with a  $2n+2$  skeletal electron count (where  $n$  is the number of vertices) is the bicapped square antiprism (**I**; Scheme 1).<sup>[1]</sup> In one of the two known isomeric forms of these

[\*] Prof. J. T. Spencer, R. Littger, U. Englisch, Dr. K. Ruhlandt-Senge  
Department of Chemistry and  
the W. M. Keck Center for Molecular Electronics  
Center for Science and Technology, Syracuse University  
Syracuse, NY 13244-4100 (USA)  
Fax: (+1) 315-443-4070  
E-mail: jtsperce@syr.edu

[\*\*] We thank the National Science Foundation (Grant Nos. CHE-9521572 and 05-27898), the Donors of the Petroleum Research Fund as administered by the American Chemical Society, the Industrial Affiliates Program of the Center for Molecular Electronics, and Syracuse University for support of this work.

Supporting information for this article is available on the WWW under <http://www.wiley-vch.de/home/angewandte/> or from the author.



Scheme 1. Structural relationship between *closo*-2-metalladecaborane (**I**) and *hypercloso*-1-metalladecaborane (**II**) clusters.

*closo*-monometalladecaborane clusters, the metal center occupies a polar in the other a tropical position. However, the alternative *hypercloso* deltahedral structure **II** was observed for some monometalladecaborane clusters. The two structural types **I** and **II** are proposed to be related by a single diamond-square (DSD) process (Scheme 1).<sup>[2c]</sup>

In our studies on the photochemistry of nonaborane organometallic derivatives of manganese, rhodium, and rhenium, we found that *nido*-borate **1**<sup>−</sup>,<sup>[3]</sup> upon irradiation, was converted in high yield into cage-unsubstituted *hypercloso*-borate **2**<sup>−</sup>, with structure **II**, by the loss of two equivalents of molecular hydrogen (Figure 1).<sup>[4]</sup> The synthesis and characterization of the two similar, albeit cage-substituted, *hypercloso* complexes **4** and **5** by different pathways was also reported previously.<sup>[2]</sup> Underivatized compounds such as **2**<sup>−</sup> and [1-( $\eta^6$ -C<sub>6</sub>Me<sub>6</sub>)Rh-*hypercloso*-B<sub>9</sub>H<sub>9</sub>]<sup>[5]</sup> provide insights into the relationship between structures **I** and **II** for cage-unsubstituted 10-vertex clusters.<sup>[6, 7]</sup> Fundamental questions remain, however, concerning the description of compounds **2–5** as either *hypercloso* 2*n* electron systems<sup>[6, 8]</sup> or as isomers of *closo* (*isocloso*) 2*n*+2 electron systems which apparently violate Wade's rules.<sup>[7]</sup>

Extended Hückel MO calculations on the model system [(CO)<sub>3</sub>RhB<sub>9</sub>H<sub>9</sub>]<sup>+/−</sup>[(CO)<sub>3</sub>RhB<sub>9</sub>H<sub>9</sub>]<sup>−</sup> showed that the bicapped square antiprismatic structure **I** is preferred for the 2*n*+2 skeletal electron count (*closo*), while the C<sub>3v</sub> structure **II** is favored for 2*n* electron systems (*hypercloso*).<sup>[8]</sup> The only

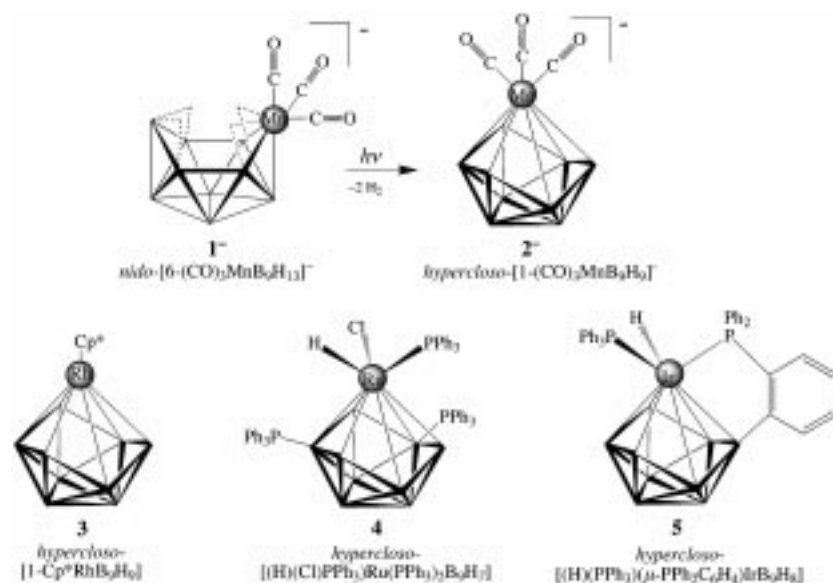
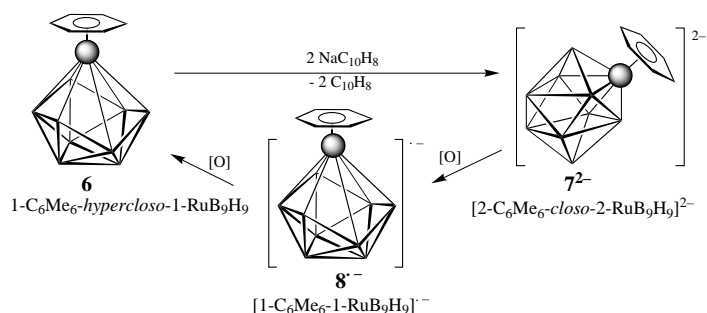


Figure 1. Photochemical generation of **2**<sup>−</sup> and structures of known *hypercloso*-nonaborane complexes (terminal hydrogen atoms omitted for clarity).

example of a *closo* to *hypercloso* conversion was reported for the reaction of **5** with CS<sub>2</sub> to yield the cage-substituted cluster [10-(PPh<sub>3</sub>)-2,6:2,9-( $\mu$ -S<sub>2</sub>CH)<sub>2</sub>-2-(*o*- $\mu$ -PPh<sub>2</sub>C<sub>6</sub>H<sub>4</sub>)-*closo*-2-IrB<sub>9</sub>H<sub>9</sub>]<sup>−</sup>.<sup>[9]</sup> An equilibrium between the *hypercloso* and *closo* forms was proposed by Hawthorne et al. for the [6-(PET<sub>3</sub>)<sub>3</sub>-*closo*-6,2,3-RuC<sub>2</sub>B<sub>7</sub>H<sub>9</sub>]/[1-(PET<sub>3</sub>)<sub>2</sub>-*hypercloso*-1,2,3-RuC<sub>2</sub>B<sub>7</sub>H<sub>9</sub>] system.<sup>[10]</sup> While a simple two-electron redox process should interconvert these structures, this has never been experimentally shown for underivatized metalladecaborane species.

Here we report the first reversible and quantitative interconversion of an unsubstituted *hypercloso*-metalladecaborane (C<sub>3v</sub> structure **II**) into the corresponding bicapped square-antiprismatic *closo*-2-metalladecaborane (structure **I**) by a simple chemical redox process (Scheme 2). The starting material **6**<sup>[5]</sup> was cleanly reduced by two equivalents of sodium



Scheme 2. Interconversion of **6** and **7**<sup>2−</sup> and the proposed intermediate radical anion species **8**<sup>2−</sup> (terminal hydrogen atoms omitted for clarity).

dihydronaphthylide to form the cage-unsubstituted complex **7**<sup>2−</sup>. This dianion was isolated in 86 % yield as pale yellow, air-sensitive disodium salts [Na(dme)]<sub>2</sub>[**7**] and [Na(thf)]<sub>2</sub>[**7**]. These compounds were characterized by NMR spectroscopy<sup>[11]</sup> and an X-ray crystal structure analysis for [Na(thf)]<sub>2</sub>[**7**].

The intensities of the signals in the one-dimensional <sup>11</sup>B NMR spectrum and the <sup>11</sup>B–<sup>11</sup>B COSY NMR correlations of **7**<sup>2−</sup> were consistent with a bicapped square-antiprismatic structure in which the metal atom occupies a tropical 2-position (C<sub>s</sub>). In addition, the NMR data of **7**<sup>2−</sup> are very similar to those reported for structurally characterized *closo*-2-metalladecaborane clusters. The <sup>11</sup>B NMR spectrum of **7** consists of six proton-coupled doublets at  $\delta$  = 35.1, −0.1, −6.1, −9.5, −26.3, and −27.9 in a 1:1:2:1:2:2 ratio. The <sup>11</sup>B chemical shift of the B(1) atom had the characteristic low-field value of  $\delta$  = +35.1, as is often observed for low-connectivity cage vertices, especially when they are adjacent to a metal center.<sup>[9]</sup>

The molecular structure of **7**<sup>2−</sup>, determined by an X-ray single-crystal analysis of [Na(thf)]<sub>2</sub>[**7**], was consistent with a structure based upon a 22-electron ten-vertex *closo*-RuB<sub>9</sub> cluster in which the metal atom occu-

pies a tropical site of a bicapped Archimedean square antiprism. The boron–boron and boron–metal distances of  $7^{2-}$  are quite typical for polyhedral *closo*-metallaboranes. The  $B_9Ru$  cage consists of a distorted square antiprismatic framework, while the ruthenium atom displays a pseudooctahedral geometry. The dianion  $7^{2-}$  is one of very few crystallographically characterized *closo*-metalladecaborane clusters and the only example that bears the same charge as the parent *closo*- $B_{10}H_{10}^{2-}$  cluster. The other related, albeit cage-substituted, examples are  $[2-(C_5H_5)-3,10-(PMe_2Ph)_2-closo-2-RhB_9H_7]$ ,<sup>[11]</sup> a subcluster in  $[(C_5Me_5)RhB_9(SMe_2)H_{10}RhB_9H_7(SMe_2)]$ ,<sup>[2a]</sup>  $[2,2-(PH_3)_2-10-(PPh_3)-2-(o-\mu-PPh_2C_6H_4)-closo-2-IrB_9H_7]^-$ ,<sup>[2b]</sup> and the analogous  $[2,10-(PPh_3)_2-2,6;2,9-(\mu-S_2CH)_2-closo-2-IrB_9H_6]$  and  $[10-(PPh_3)_2-2,6;2,9-(\mu-S_2CH)_2-2-(o-\mu-PPh_2C_6H_4)-closo-2-IrB_9H_6]^-$ .<sup>[9]</sup> Also related are heterometallic clusters such as *closo*- $[2,2,2-(PMe_3)_2H-2,1-IrSB_8H_8]$ .<sup>[12]</sup>

Interestingly, the relatively stable radical anion intermediate  $8^{\cdot-}$  was observed on one-electron oxidation of  $7^{2-}$ . The  $^{11}B$  NMR spectrum of  $8^{\cdot-}$  consists of proton-coupled doublets at  $\delta = 90.0$ , 21.5, and  $-14.2$  in a 1:1:1 ratio. On the basis of spectroscopic data,  $8^{\cdot-}$  is believed to have a  $C_{3v}$  structure related to that of the *hypercloso*-cluster **6**. The complex also displayed a broad, unresolved signal in the EPR spectrum. Further oxidation of  $8^{\cdot-}$  converted it quantitatively into the *hypercloso*-complex **6**.

This is the first example of a chemically reversible *hypercloso*–*closo*–*hypercloso* redox interconversion and further represents the first *hypercloso*–*closo* process of a noncage substituted compound. We are currently exploring the structure and chemistry of the radical anion intermediate  $8^{\cdot-}$ .

### Experimental Section

$[Na(dme)_2][7]$ : Under a nitrogen atmosphere, a dry, degassed 0.10 M solution of sodium dihydronaphthylide in dimethoxyethane (DME) was slowly added to a suspension of **6**<sup>[5]</sup> (130 mg, 0.35 mmol) in dry, degassed DME (20 mL) at  $-40^\circ C$ , during which time **6** completely dissolved. Addition of the reducing agent was stopped when its dark green color persisted in solution (approximately 7 mL).  $^{11}B$  NMR spectroscopy showed complete conversion of **6** to  $[Na(dme)_2][7]$ . The solution was then slowly warmed to room temperature, during which time a precipitate was formed, and stored overnight at  $15^\circ C$ . The solid was filtered off, washed with 2 mL of dry, degassed DME and dried in vacuo.  $[Na(dme)_2][7]$  was obtained as a pale yellow, air-sensitive solid (180 mg, 86.4% yield). The salt is only slightly soluble in THF and DME, more soluble in  $CH_3CN$ , and very soluble in water (degassed).  $^{11}B$  NMR (96.3 MHz,  $CD_3CN$ ):  $\delta = 35.1$  (d,  $^1J_{BH} = 137$  Hz, 1B, B(1)),  $-0.1$  (d,  $^1J_{BH} = 138$  Hz, 1B, B(10)),  $-6.1$  (d,  $^1J_{BH} = 107$  Hz, 2B, B(6,7)),  $-9.5$  (d,  $^1J_{BH} = 116$  Hz, 1B, B(4)),  $-26.3$  (d,  $^1J_{BH} = 110$  Hz, 2B, B(3,5)),  $-27.9$  (d,  $^1J_{BH} = 126$  Hz, 2B, B(8,9));  $^{11}B$ – $^{11}B$  COSY NMR correlations: 1 (4, 3, 5), 10 (6, 7, 8, 9), 6, 7 (10, 3, 5), 4 (1, 8, 9), 3, 5 (1, 6, 7), 8, 9 (10, 4);  $^1H$  [ $^{11}B$ ] NMR (300.1 MHz,  $CD_3CN$ ):  $\delta = 4.97$  (s,  $BH_{exo}$ ), 3.47 (s, 8H,  $H_3COCH_2$ ), 3.29 (s, 12H,  $H_3COCH_2$ ), 1.88 (s, 18H,  $C_6(CH_3)_6$ ), 3.01 (s,  $BH_{exo}$ ),  $-0.99$  (s,  $BH_{exo}$ ),  $-1.16$  (s,  $BH_{exo}$ ). X-ray structure analysis of  $[Na(thf)_2][7]$ :<sup>[13]</sup> Siemens SMART CCD diffractometer,  $MoK_\alpha$  radiation,  $C_{28}H_{39}B_9Na_2O_4Ru$  ( $M_r = 704.09$ ), monoclinic, space group  $P2_1/c$ ,  $a = 19.2595(1)$ ,  $b = 13.8368(1)$ ,  $c = 13.7534(2)$  Å,  $\beta = 90.244(1)^\circ$ ,  $V = 3665.08(6)$  Å<sup>3</sup>,  $Z = 4$ ,  $\rho_{calcd} = 1.276$  g cm<sup>-3</sup>.

$[Na(thf)_2][7]$  was prepared in an identical fashion to  $[Na(dme)_2][7]$ , except that THF was substituted for DME. The THF-solvated compound was employed here since it was more soluble in ether solvents and gave superior crystals. Pale yellow crystals of  $[Na(thf)_2][7]$  were grown from a saturated solution in THF/hexane at  $-15^\circ C$ . The crystals were removed from the Schlenk tube under a stream of inert gas and immediately covered with a layer of viscous hydrocarbon oil. A suitable crystal was selected under the

microscope, attached to a glass fiber and immediately placed in the low-temperature nitrogen stream of the diffractometer.<sup>[13, 14]</sup> The data collection covered over a hemisphere of reciprocal space by a combination of three sets of exposures. Each exposure covered  $0.3^\circ$  in  $\omega$ . Crystal decay was monitored by repeating the initial frames at the end of data collection and analyzing the duplicate reflections. No decay was observed.  $T = 150(2)$  K,  $2.12 \leq 2\theta \leq 56.40$ ; 29272 reflections measured, of which 8590 were unique and 7485 observed ( $I > 2\sigma(I)$ ). Solution: direct methods. Full-matrix refinement on  $F_o^2$  (SHELXL93); empirical absorption correction applied (SADABS). Four THF solvent molecules and the hydrogen atoms of the boron cage were located in the difference map and were refined with free coordinates and displacement parameters; 453 parameters,  $wR_2 = 0.0731$  for all data,  $R_1 = 0.0292$  ( $I > 2\sigma(I)$ ). Crystallographic data (excluding structure factors) for the structure reported in this paper have been deposited with the Cambridge Crystallographic Data Centre as supplementary publication no. CCDC-138294. Copies of the data can be obtained free of charge on application to CCDC, 12 Union Road, Cambridge CB2 1EZ, UK (fax: (+44) 1223-336-033; e-mail: deposit@ccdc.cam.ac.uk).

Oxidation of  $[Na(dme)_2][7]$ : Under an inert atmosphere, a sample of the complex in dry, degassed  $CD_3CN$  was exposed to the air by removal of the stopper for 1 s. The tube was then resealed. The initial pale yellow color of  $7^{2-}$  turned red. The  $^{11}B$  NMR spectrum of this solution showed, besides signals for **6** and  $7^{2-}$ , three new signals at  $\delta = 90.0$ , 21.5, and  $-14.2$  (1:1:1). Upon further exposure to the air, the  $^{11}B$  NMR spectrum showed signals only for the completely oxidized complex **6** ( $\delta = 94.6$ , 27.9, and  $-12.3$ ).

Received: July 9, 1999 [Z13701]

- [1] a) K. Wade, *J. Chem. Soc. Chem. Commun.* **1971**, 792; b) D. M. P. Mingos, *Nature (London) Phys. Sci.* **1972**, 236, 99.
- [2] a) E. J. Ditzel, X. L. R. Fontaine, N. N. Greenwood, J. D. Kennedy, M. Thornton-Pett, *J. Chem. Soc. Chem. Commun.* **1989**, 1262; b) J. Bould, N. N. Greenwood, J. D. Kennedy, M. Thornton-Pett, *J. Chem. Soc. Chem. Commun.* **1982**, 465; c) J. E. Crook, M. Elrington, N. N. Greenwood, J. D. Kennedy, M. Thornton-Pett, J. D. Woollins, *J. Chem. Soc. Dalton Trans.* **1985**, 2407.
- [3] J. W. Lott, D. F. Gaines, *Inorg. Chem.* **1974**, 13, 2261.
- [4] R. Littger, J. T. Spencer, unpublished results. Spectroscopic data for compound **2**:  $^{11}B$  NMR:  $\delta = +110$  (d, 3B,  $J_{BH} = 153$  Hz, B(2,3,4)),  $+28.4$  (d, 3B,  $J_{BH} = 135$  Hz, B(8,9,10)),  $-14.8$  (d, 3B,  $J_{BH} = 139$  Hz, B(5,6,7)).
- [5] E. J. Ditzel, X. L. R. Fontaine, N. N. Greenwood, J. D. Kennedy, M. Thornton-Pett, *Z. Anorg. Allg. Chem.* **1992**, 616, 79.
- [6] R. T. Baker, *Inorg. Chem.* **1986**, 25, 109.
- [7] J. D. Kennedy, *Inorg. Chem.* **1986**, 25, 111.
- [8] a) R. L. Johnson, D. P. M. Mingos, *Inorg. Chem.* **1986**, 25, 3321; b) R. L. Johnson, D. P. M. Mingos, *New J. Chem.* **1991**, 15, 831.
- [9] R. S. Coldicott, J. D. Kennedy, M. Thornton-Pett, *J. Chem. Soc. Dalton Trans.* **1996**, 3819.
- [10] C. W. Jung, R. T. Baker, M. F. Hawthorne, *J. Am. Chem. Soc.* **1981**, 103, 810.
- [11] X. L. R. Fontaine, H. Fowkes, N. N. Greenwood, J. D. Kennedy, M. Thornton-Pett, *J. Chem. Soc. Dalton Trans.* **1987**, 1431.
- [12] J. Bould, N. P. Rath, L. Barton, *Organometallics* **1996**, 15, 4916.
- [13] Data Collection; SMART Software Reference Manual (1994), Siemens Analytical X-ray Instruments. Data reduction; SAINT Version 4 Software Reference Manual (1995), Siemens Analytical X-ray Instruments. Structure Solution, Refinement and Graphics: G. M. Sheldrick (1994), SHELXTL Version 5 Reference Manual, Siemens Analytical X-ray Instruments. Neutral atom scattering factors: *International Tables for Crystallography, Vol. C*, Kluwer, Boston, **1995**, Tables 6.1.1.4, 4.2.6.8, and 4.2.4.2. Program for Absorption Correction Using Area Detector Data (SADABS), G. M. Sheldrick, University of Göttingen, Germany, **1996**.
- [14] H. Hope, *Prog. Inorg. Chem.* **1994**, 41, 1.